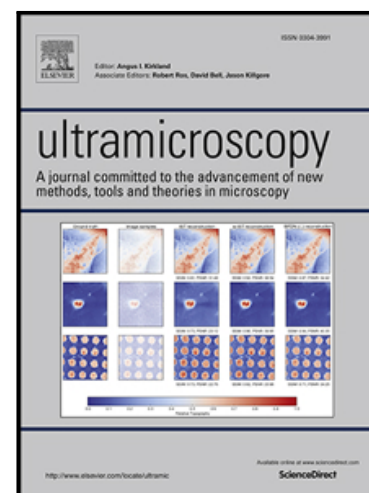


Accepted Manuscript

In situ atomic scale mechanisms of strain-induced twin boundary shear to high angle grain boundary in nanocrystalline Pt

Lihua Wang , Jiao Teng , Yu Wu , Xuechao Sha , Sisi Xiang , Shengcheng Mao , Guanghua Yu , Ze Zhang , Jin Zou , Xiaodong Han

PII: S0304-3991(18)30040-8
DOI: <https://doi.org/10.1016/j.ultramic.2018.08.022>
Reference: ULTRAM 12640



To appear in: *Ultramicroscopy*

Received date: 10 February 2018
Revised date: 16 August 2018
Accepted date: 26 August 2018

Please cite this article as: Lihua Wang , Jiao Teng , Yu Wu , Xuechao Sha , Sisi Xiang , Shengcheng Mao , Guanghua Yu , Ze Zhang , Jin Zou , Xiaodong Han , In situ atomic scale mechanisms of strain-induced twin boundary shear to high angle grain boundary in nanocrystalline Pt, *Ultramicroscopy* (2018), doi: <https://doi.org/10.1016/j.ultramic.2018.08.022>

This is a PDF file of an unedited manuscript that has been accepted for publication. As a service to our customers we are providing this early version of the manuscript. The manuscript will undergo copyediting, typesetting, and review of the resulting proof before it is published in its final form. Please note that during the production process errors may be discovered which could affect the content, and all legal disclaimers that apply to the journal pertain.

In situ atomic scale mechanisms of strain-induced twin boundary shear to high angle grain boundary in nanocrystalline Pt

Lihua Wang^{1*}, Jiao Teng², Yu Wu², Xuechao Sha¹, Sisi Xiang¹, Shengcheng Mao¹, Guanghua Yu², Ze Zhang³, Jin Zou⁴ and Xiaodong Han^{1*}

¹Beijing Key Lab of Microstructure and Property of Advanced Material, Institute of Microstructure and Properties of Advanced Materials, Beijing University of Technology, Beijing, 100124, China

²Department of Material Physics and Chemistry, University of Science and Technology Beijing, Beijing 100083, China

³Department of Materials Science, Zhejiang University, Hangzhou, 310008, China

⁴Materials Engineering and Centre for Microscopy and Microanalysis, The University of Queensland, Brisbane, QLD 4072, Australia

* Corresponding author: wlh@bjut.edu.cn; xdhan@bjut.edu.cn;

Twin boundary can both strengthen and soften nanocrystalline metals and has been an important path for improving the strength and ductility of nano materials. Here, using in-lab developed double-tilt tensile stage in the transmission electron microscope, the atomic scale twin boundary shearing process was *in situ* observed in a twin-structured nanocrystalline Pt. It was revealed that the twin boundary shear was resulted from partial dislocation emissions on the intersected {111} planes, which accommodate as large as 47% shear strain. It is uncovered that the partial dislocations nucleated and glided on the two intersecting {111} slip planes lead to a transition of the original <110> symmetric tilt $\Sigma 3/(111)$ coherent twin boundary into a <110> symmetric tilt $\Sigma 9/(114)$ high angle grain boundary. These results provide insight of twin boundary strengthening mechanisms for accommodating plasticity strains in nanocrystalline metals.

Key words: atomic scale; *in situ*; grain boundary structure transition; shear strain; twin

1. Introduction

The mechanical properties of polycrystalline materials depend on the transmission of forces and fields across their grain boundaries (GBs) [1-2], and can be sensitive to the GB structures. During the plastic deformation, structural transitions at GBs always take place, and in turn can lead to the change of mechanical properties of polycrystalline materials (such as strength, ductility) [1-3]. Revealing the atomic-scale mechanism of how GBs accommodate large plasticity is crucial for understanding the performance of polycrystalline materials, since it can provide guidance to design the desired mechanical properties. Especially for the twin boundaries (TBs), the atomic-scale mechanism of how they accommodate large plasticity has been a global research focus for many years, which attribute to the fact that the twin-structured metals exhibit not only ultrahigh strength, but also considerable ductility [4,5]. It is well documented that the TBs are the effective obstruction to the dislocation motion, and the TBs are also stable against sliding or diffusion (both leading to softening) than the conventional GBs. These factors lead to the twin-structured metals exhibiting ultrahigh strength [4-8]. This strengthening mechanism, resulted from the TBs interaction with the dislocations, is clearly revealed by post-mortem transmission electron microscopy (TEM) investigations [5,9,10] and also confirmed by the molecular dynamic simulations [4,11-17]. While for the ultrahigh ductility mechanisms of twin-structured metals, why those TBs can accommodate ultra-large plastic strain without any crack or void initiation, and how the TBs accommodate during the dislocation emission and twin nucleation are still unclear because of lacking of *in situ* observations at atomic level [18,19]. It is therefore of interest to understand the atomic scale process of how a TB accommodates the plastic strain during loading. However, a direct atomic-scale observation of how a TB accommodates the large plastic strain is a challenging experiment [20-24].

Here, by employing our home-made double-tilt tensile stage in a TEM [22,25,26], the atomic-scale deformation process of the nanocrystalline (NC) platinum (Pt) thin film was *in situ* captured. The atomic scale dynamic processes of partial dislocations nucleation from TBs and gliding on the two sets of $\{111\}$ planes were directly observed in the twin-structured nanometer grains. We uncovered that the successive nucleation and motion of these partial dislocations lead to a new twin nucleation and a transition of $\Sigma 3/(111)$ TB into a $\Sigma 9/(114)$

high-angle grain boundary (HAGB). This is the direct evidence to demonstrate a TB accommodating ultra-large plastic strain by a GB structure transformation.

2. Experimental

The NC Pt thin film with a thickness of 15 nm was deposited on a (001)-oriented NaCl single-crystal substrate ($3 \times 3 \text{ cm}^2$) at 300°C by magnetron sputtering. For TEM observations, the NC Pt thin film was removed from the NaCl substrate by dissolving the NaCl substrate in purified water. TEM investigations showed that the NC Pt thin film consists nano-sized and equiaxed grains without obvious preferred orientation and most grains are separated by HAGBs. The grain diameters (d) ranged from 4 to 20 nm and most of the grains had diameter below 15 nm, giving rise to an average d of 10nm [25]. With our newly developed double-tilt TEM tensile stage [22,25,26], the NC Pt thin film was slowly and gently deformed inside a JEOL-2010 field emission TEM operating at 200 kV. The double-tilt capability of our TEM tensile stage allows the strained grains to be oriented conveniently for high-resolution TEM (HRTEM) imaging, so that the deformation process can be monitored at the atomic scale during the tensile loading. The real-time evolution of the film was captured *in situ* along with its deformation inside the TEM.

3. Atomic model illustrates how TBs accommodate shear strain

In order to distinguish the classic twin nucleation mechanisms and the current experimental observations, we illustrate the classic twinning model together with the current observation of TB shear processes. Based on the classic twinning model in face-centered cubic (FCC) metals, a deformation twin is normally formed through the glide of Shockley partial dislocations on successive $\{111\}$ planes that produce large shear strain. Fig. 1a illustrates that the FCC metal can emit three equivalent Shockley partials with Burgers vectors of $\mathbf{b} = 1/6\langle 112 \rangle$ on each $\{111\}$ planes. Taken the $(\bar{1}\bar{1}\bar{1})$ slip plane as an example, the three equivalent Shockley partial dislocations have their Burgers vectors of $\mathbf{b}_1 = 1/6[\bar{1}2\bar{1}]$, $\mathbf{b}_2 = 1/6[2\bar{1}\bar{1}]$ and $\mathbf{b}_3 = 1/6[\bar{1}\bar{1}\bar{2}]$. The \mathbf{b}_1 and \mathbf{b}_2 are 30° partial dislocations with screw component along the $[\bar{1}\bar{1}0]$ direction, and \mathbf{b}_3 is a 90° partial dislocation with pure edge component along the $[\bar{1}\bar{1}\bar{2}]$ direction. If the twin formed by 30° partial dislocations \mathbf{b}_1 or \mathbf{b}_2 gliding on the $(\bar{1}\bar{1}\bar{1})$ plane, the GB kink angle is 164.3° as shown in Fig. 1c. When the twin formed by 90° partial dislocations \mathbf{b}_3 , the GB kink angle is 141° as shown in Fig. 1d. It should

be noted that the deformation twin can also be formed by three equivalent partial dislocations, i.e. $b_4=1/6[\bar{2}11]$, $b_5=1/6[\bar{1}2\bar{1}]$ and $b_6=1/6[1\bar{1}2]$ gliding on (111) planes. As indicated in the Fig. 1e and Fig. 1f, the GB kink angle is 164.2° if the twin is formed by 30° partial dislocations b_4 or b_5 , and the GB kink angle is 141° while the twin is formed by 90° partial dislocations b_6 . Based on the models outlined above, we can see that the GB kink angle of the deformation twin can be served as a reference of the twinning model and dislocation types (90° or 30° partial dislocations). We can then analyze the experimentally observed twinning model by comparing the measured GB kink angles with those predicted by the theoretical twinning models. For example, the twinning mode with zero macroscopic strain were observed experimentally in NC metals since the GB kink angle is zero [27]. In our experimental observation, the GB kink angle of the deformation twin is 144.9° , neither 141° nor 164.2° . The twinning process was involved partial dislocations that glide on two intersecting {111} slip planes as revealed by the subsequent sessions.

4. *In situ* atomic-scale observation of the TB-HAGB transition

Figs. 2a-f provide a series of $[\bar{1}10]$ zone-axis HRTEM images captured *in situ* showing atomic-scale evolution of the TB-HAGB transition process in a twin-structured grain, from which the new twin nucleation and growth process can be revealed directly. During the deformation, there is no obvious orientation change in T1 and T2, indicating that there is no global tilt of the specimen during the deformation. As can be seen from Fig. 2a, the TB of the twin-structured grains is flat. Under the loading, a new twin with a 3-layer thick is formed in T1, leading to a splitting of the flat TB1 between TB1 and TB2. Simultaneously, a deformation twin (marked as T3) with a width of 3 atomic layers is formed in T1 and the original flat TB is kinked and changed into a new GB, as marked in Fig. 2b. Since the measured misorientation angle between the T3 and T1 is $\sim 43.6^\circ$, thus, the newly formed GB is a HAGB. With further loading, both the width of the deformation twin and the length of HAGB increase quickly, resulting in an ultra-large shear strain toward the right side. Fig. 2c-f display a series of captured HRTEM images from the same region, showing the twin growth from 5 atomic layers into 6 atomic layers, and then tens of atomic layers (Fig. 2e, Fig. 2f), which is caused by the nucleation and forward propagation of partial dislocations emitted from the TB in a fashion of layer-by-layer. Figs. 2g-i show the enlarged HTEM images

corresponding to the red framed regions of Fig. 2b, c and e, respectively, showing the atomic structure of the deformation twin more clearly.

To reveal how the TBs accommodate the ultra-large shear strain in more details, Figs. 3a-c provide the enlarged HRTEM images and show the TB-HAGB transition process more clearly. As shown in Fig. 3a and 3b, as the 3-layered twin nucleated in T1, the original flattened TB changes into a typical HAGB. It is of interest to note that, with the growth of the new twin, the TB2 also undergoes a migration process and the number of the migration layer is always equal to the number of atomic layers associated with the twin. As can be seen from Fig. 3b and 3c, the new twin grows from 3 atomic layers into 6 atomic layers, while the number of the migration layer for TB1 is 3 atomic layers at the beginning and becomes to 6 atomic layers later. It is obvious that the new twin nucleation and the TB migration process takes place at the same time, indicating that there are two partial dislocation activities during the deformation. One of the dislocation activities is that the partial dislocations nucleated glide on the successive (111) planes of TB2 that is parallel to the TB2, leading to the TB migration. Another dislocation activity is that the partial dislocations nucleated in T1 glide on the successive $(\bar{1}\bar{1}1)$ plane that is inclined with the TB, resulting in a new twin nucleation. These two dislocation activities lead to the TB transition into a symmetric tilt HAGB.

By carefully analyzing the shear direction (along the [112] direction) and the GB kink angle (measured as 144.9°), we anticipate that the new twin is resulted from 30° partial dislocations with $b_1=1/6[1\bar{2}1]$ or $b_2=1/6[2\bar{1}1]$ that glide on the successive $(\bar{1}\bar{1}1)$ planes (the 90° partial dislocations can be excluded). Additionally, considering the HAGB structure and the obvious shear along $[\bar{1}\bar{1}2]$ direction, the TB migration should be resulted from the 30° partial dislocation with $b_4=1/6[\bar{2}11]$ or $b_5=1/6[1\bar{2}1]$ that must glide on the successive (111) planes. During the TB-HAGB transition process, the atomic-scale structure of HAGB can be clearly seen with no obvious angle deviation. This indicates that the out of plane tilt caused by the screw component of these 30° partial dislocations is cancelling out via the dislocation reactions. Thus, the dislocation emission process during the TB-HAGB transition can be written as follows:

$$b_1 + b_5 = \frac{1}{\sqrt{6}} [\bar{1}10] + \frac{1}{\sqrt{6}} [2\bar{1}\bar{1}] = \frac{1}{\sqrt{6}} [1\bar{1}0] \quad (1)$$

$$\text{Or } b_2 + b_4 = \frac{1}{6} [2\bar{1}\bar{1}] + \frac{1}{6} [2\bar{1}\bar{1}] = \frac{1}{3} [001] \quad (2)$$

Figs. 3d-f show the atomic configurations illustrating the dislocation nucleation and motion process. Before the plastic deformation, the TB is flat, as shown in Fig. 3d. During the deformation, as indicated in Fig. 3e, two partial dislocations on two intersecting slip planes nucleated and interacted with each other. The partials b_1 or b_2 nucleated from the TB glide on the $(\bar{1}\bar{1}1)$ slip plane (inclined with the TB) which results in a stacking fault. At the meaning time, the partials b_4 or b_5 nucleated from the same sites glide on the (111) plane, leading to the TB migration. Repetition of above partial dislocation activities leads to the new twin nucleation and the transition from the TB into a HAGB, as shown in Fig. 3f.

Fig. 4a illustrates a typical HRTEM image showing the atomic-scale structure of the newly formed HAGB. The angle of (001) or (110) planes across the newly formed HAGB was measured to be 43.6° . Based on the previous theoretical model [28,29], this GB segment should be a $\Sigma 9$ boundary with a misorientation angle of 38.9° . However, our measured misorientation angle is $\sim 4.7^\circ$ larger than the theoretical value. This may be due to the local stress concentration caused by the lattice distortion. Fig. 4b displays an enlarged HRTEM image and shows the atomic-scale structure of the HAGB. Detailed analysis reveals that the structural unit is different from the theoretic $\Sigma 9/(114)$ GB structure [28], as shown in Fig. 4c. Besides the local lattice distortion, the localized stacking fault configurations can also impact the GB structure. In particular, as the stacking fault energy of Pt is high, the observed structural unit can be different from the theoretic prediction.

Here, the shear strain along the $[112]$ direction of T2 (as marked in Fig. 4a) is contributed from the partial dislocation behaviors on both the $(\bar{1}\bar{1}1)$ and (111) planes. These 30° partial dislocations only produce a displacement of $a\sqrt{6}/12$ because their Burgers vector \mathbf{b} has a 30° angle with the viewed $[\bar{1}10]$ zone-axis. Based on the above described dislocation activities, the shear strain can be estimated as $\sim 47\%$, according to the formula

$$\varepsilon = \left(\frac{a\sqrt{6}}{12} + \frac{a\sqrt{6}}{12} \cos 70.5^\circ \right) / \frac{a\sqrt{3}}{3}.$$

Although this twinning model has been proposed previously [29], there is no direct experimental evidence to prove this is indeed the case. In this study, we provide the first *in situ* atomic scale observation of TB shear process in a twin-structured NC Pt. The results show that the atomic-structure and the mis-orientation angle of the newly nucleated HAGB is different from that predicted the theoretical model [28]. Additionally, unlike the theoretical model proposal that the formation of secondary twin is resulted from the 90° partial dislocation [29], our results demonstrated that the TB shear is resulted from 30° partial dislocations, which produce less shear strain (along the [112] direction) than the 90° partial dislocations.

In polycrystalline or NC materials, the formed micro-crack can directly lead to the materials failure even their formation probability is very low as compared with dislocation and twinning. For example, as proposed both by experimental tests [30-32] and molecular dynamics simulations [33-37], the mismatch and large shear strain usually induce high stress concentration at the intersections of twins and conventional GBs during twinning, which leads to fracture or cracks during the plastic deformation. Thus, TB can accommodate large local strain without micro-crack formation, which is a pre-request of high ductility of twin structured materials. Here, our *in situ* atomic-scale dynamic observations show that the TB can accommodate as large as 47% shear strain by the TB-HAGB transition, no crack was initiated during the twinning process. These demonstrate that the high compatible ability of TBs may be one of the important factors for the high ductility of the twin structured metals, especially for those metals with low stacking fault energy such as Cu, Ag and Au [4,7,38-41].

In conclusion, with the aid of our newly developed tensile stage, the atomic-scale TB-HAGB transition process is directly observed in HRTEM. The GB structure transition is realized by the partial glide on two intersecting {111} slip planes, which eventually leads to the transition of an original <110> symmetric tilt $\Sigma 3/(111)$ coherent TB into a <110> symmetric tilt $\Sigma 9/(114)$ HAGB. During the TB-HAGB transition, the TB can accommodate as large as 47% shear strain without initiating cracks. This study sheds light for fundamentally

understanding the deformation mechanisms and high ductility of twin-structured NC metals, and also have implications for new opportunities to achieve metals with desired high strength and large ductility.

Acknowledgements

This work was supported by the National Key R & D Program of China (2017YFB0305501); the National Science Fund for Excellent Young Scholars (11722429), the Key Project of NSFC (11234011), the NSFC (51771104, 11374030, 11327901), China, the Fok Ying-Tong Education Foundation of China (151006).

References:

- [1] B. Straumal, B. Baretzky, Grain boundary phase transitions and their influence on properties of polycrystals, *Interf. Sci.* 12 (2004) 147-155.
- [2] P.L. Liu, J.K. Shang, Interfacial embrittlement by bismuth segregation in copper/tin-bismuth Pb-free solder interconnect, *J. Mater. Res.* 16 (2001) 1651-1659.
- [3] H.F. Wang and Y.M. Chiang, Thermodynamic stability of intergranular amorphous films in bismuth-doped Zinc oxide, *J. Am. Ceram. Soc.* 81 (1998) 89-96.
- [4] L. Lu, X. Chen, X. Huang, K. Lu, Revealing the maximum strength in nanotwinned copper, *Science* 323 (2009) 607-610.
- [5] L.H. Wang, Y. Lu, D.L. Kong, L.R. Xiao, X.C. Sha, J.L. Sun, Z. Zhang, X.D. Han, Dynamic and atomic-scale understanding of the twin thickness effect on dislocation nucleation and propagation activities by in situ bending of Ni nanowires, *Acta Mater.* 90 (2015) 194-203.
- [6] X.Y. Li, Y.J. Wei, L. Lu, K. Lu, H.J. Gao, Dislocation nucleation governed softening and maximum strength in nano-twinned metals, *Nature* 464 (2010) 877-880.
- [7] E. Ma, Y.M. Wang, Q.H. Lu, M.L. Sui, L. Lu, K. Lu, Strain hardening and large tensile elongation in ultrahigh-strength nano-twinned copper, *Appl. Phys. Lett.* 85 (2004) 4932-4934.
- [8] C.J. Shute, B.D. Myers, S. Xie, T.W. Barbee, Jr., A.M. Hodge, J. R. Weertman, Microstructural stability during cyclic loading of multilayer copper/copper samples with nanoscale twinning, *Scripta Mater.* 60 (2009) 1073-1077.

- [9] J.W. Christian, S. Mahajan, deformation twinning, *Prog. Mater. Sci.* 39 (1995) 1-57.
- [10] Y.B. Wang, M.L. Sui, E. Ma, In situ observation of twin boundary migration in copper with nanoscale twins during tensile deformation, *Phil. Mag. Lett.* 87 (2006) 935-942.
- [11] A.G. Frøseth, P.M. Derlet, H. Van Swygenhoven, Grown-in twin boundaries affecting deformation mechanisms in nc-metals, *Appl. Phys. Lett.* 85 (2004) 5863-5865.
- [12] H. Van Swygenhoven, P.M. Derlet, A.G. Frøseth, Stacking fault energies and slip in nanocrystalline metals, *Nature Mater.* 3 (2004) 399-403.
- [13] G.P. Zheng, Y.M. Wang, M. Li, Atomistic simulation studies on deformation mechanism of nanocrystalline cobalt, *Acta Mater.* 53 (2005) 3893-3901.
- [14] T. Zhu, J. Li, A. Samanta, H. G. Kim, S. Suresh, Interfacial plasticity governs strain rate sensitivity and ductility in nanostructured metals, *Proc. Natl. Acad. Sci. U.S.A.* 104 (2007) 3031-3036.
- [15] Y.J. Wei, The kinetics and energetic of dislocation mediated de-twinning in nano-twinned face-centered cubic metals. *Mater. Sci. Eng. A.* 528 (2008) 1558-1566.
- [16] I. Shabib and R. E. Miller, Deformation characteristics and stress-strain response of nanotwinned. Cu, *Acta Mater.* 57 (2009) 4364-4373.
- [17] A. Stukowski, K. Albe, Nanotwinned fcc metals: strengthening versus softening mechanisms, *Phys. Rev. B* 82 (2010) 224103.
- [18] S. Pathak, J. Michler, K. Wasmer, S. R. Kalidindi, Studying grain boundary regions in polycrystalline materials using spherical nano-indentation and orientation imaging microscopy, *J. Mater. Sci.* 47 (2012) 815-823.
- [19] L.H. Wang, J. Teng, X.C. Sha, J. Zou, Ze Zhang, X.D. Han, Plastic deformation through dislocation saturation in ultrasmall Pt nanocrystals and its in situ atomistic mechanisms, *Nano Lett.* 17 (2017) 4733-4739.
- [20] M.A. Haque, M.T.A. Saif, Deformation mechanisms in free-standing nanoscale thin films: A quantitative in situ transmission electron microscope study, *Proc. Natl. Acad. Sci. U.S.A.* 101 (2004) 6335-6340.
- [21] L.H. Wang, P. Liu, P.F. Guan, M.J. Yang, J.L. Sun, Y.Q. Cheng, A. Hirata, Z. Zhang, E. Ma, M.W. Chen, X.D. Han, In situ atomic-scale observations of continuous and reversible lattice deformation far beyond the elastic limit, *Nat. Commun.* 4 (2013) 2413.

- [22] L.H. Wang, X.D. Han, Z. Zhang, In situ experimental mechanics of nanomaterials at the atomic scale, *NPG Asia Mater.* 5 (2013) e40.
- [23] V. Yamakov, D. Wolf, S.R. Phillpot, A.K. Mukherjee, H. Gleiter, Deformation-mechanism map for nanocrystalline metals by molecular-dynamics simulation, *Nat. Mater.* 3 (2004) 43-47.
- [24] D. Wolf, V. Yamakov, S.R. Phillpot, A. Mukherjee, H. Gleiter, Deformation of nanocrystalline materials by molecular-dynamics simulation: relationship to experiments?, *Acta Mater.* 53 (2005) 1-40.
- [25] L.H. Wang, X.D. Han, P. Liu, Y.H. Yue, Z. Zhang, E. Ma, In situ observation of dislocation behavior in nanometer grains, *Phys. Rev. Lett.* 105 (2010) 135501.
- [26] L.H. Wang, Z. Zhang, E. Ma, X. D Han, Transmission electron microscopy observations of dislocation annihilation and storage in nanograins, *Appl. Phys. Lett.* 98 (2010) 051905.
- [27] Y.T. Zhu, X.Z. Liao, X.L. Wu, Deformation twinning in nanocrystalline, *Prog. Mater. Sci.* 57 (2012) 1-62.
- [28] J.D. Rittner, D.N. Seidman, $\langle 110 \rangle$ symmetric tilt grain-boundary structures in fcc metals with low stacking-fault energies, *Phys. Rev. B* 54 (1996) 6999-7015.
- [29] Y.T. Zhu, X.Z. Liao, R.Z. Valiev, Formation mechanism of fivefold deformation twins in nanocrystalline face-centered-cubic metals, *Appl. Phys. Lett.* 86 (2005) 103112.
- [30] B.C. Ng, B.A. Simkin, M.A. Crimp, T.R. Bieler, The role of mechanical twinning on microcrack nucleation and crack propagation in a near- γ TiAl alloy, *Intermetallics* 12 (2004) 1317-1323.
- [31] B.A. Simkin, B.C. Ng, M.A. Crimp, T.R. Bieler, Crack opening due to deformation twin shear at grain boundaries in near- γ TiAl, *Intermetallics* 15 (2007) 55-60.
- [32] L.H. Wang, P.F. Guan, J. Teng, P. Liu, D.K. Chen, W.Y. Xie, D.L. Kong, S.B. Zhang, T. Zhu, Z. Zhang, E. Ma, M.W. Chen, X.D. Han, New twinning route in face-centered cubic nanocrystalline metals, *Nat. Commun.* 8 (2017) 2142.
- [33] Q.H. Tang, T.C. Wang, Deformation twinning and its effect on crack extension, *Acta Mater.* 46 (1998) 5313-5321.
- [34] V. Yamakov, E. Saether, D.R. Phillips, E.H. Glaessgen, Molecular-dynamics simulation-based cohesive zone representation of intergranular fracture processes in

aluminum, *J. Mech. Phys. Solids* 54 (2004) 1899-1928.

[35] Y.F. Zhang, P.C. Millett, M. Tonks, B. Biner, Deformation-twin-induced grain boundary failure, *Scripta Mater.* 66 (2012) 117-120.

[36] S.V. Bobylev, N.F. Morozov, I.A. Ovid'ko, Cooperative grain boundary sliding and nanograin nucleation process in nanocrystalline, ultrafine-grained, and polycrystalline solids, *Phys. Rev. B* 84 (2011) 094103.

[37] I.A. Ovid'ko, A.G. Sheinerman, E.C. Alfantis, Stress-driven migration of grain boundaries and fracture processes in nanocrystalline ceramics and metals, *Acta Mater.* 56 (2008) 2718-2727.

[38] L.H. Wang, D.L. Kong, Y. Zhang, L.R. Xiao, Y. Lu, Z.G. Chen, Z. Zhang, J. Zou, T. Zhu, X.D. Han, Mechanically driven grain boundary formation in nickel nanowires, *ACS Nano* 11 (2017) 12500-12508.

[39] L. Lu, Y.F. Shen, X.H. Chen, L.H. Qian, K. Lu, Ultrahigh strength and high electrical conductivity in copper, *Science* 304 (2004) 422-426.

[40] J.H. Seo, H.S. Park, Y. Yoo, T.Y. Seong, J. Li, J.P. Ahn, B. Kim, I.S. Choi, Origin of size dependency in coherent-twin-propagation-mediated tensile deformation of noble metal nanowires, *Nano Lett.* 13 (2013) 5112-5116.

[41] X.Z. Liao, S.G. Srinivasan, Y.H. Zhao, M.I. Baskes, Y.T. Zhu, Formation mechanism of wide stacking faults in nanocrystalline Al, *Appl. Phys. Lett.* 84 (2004) 3564-3566.

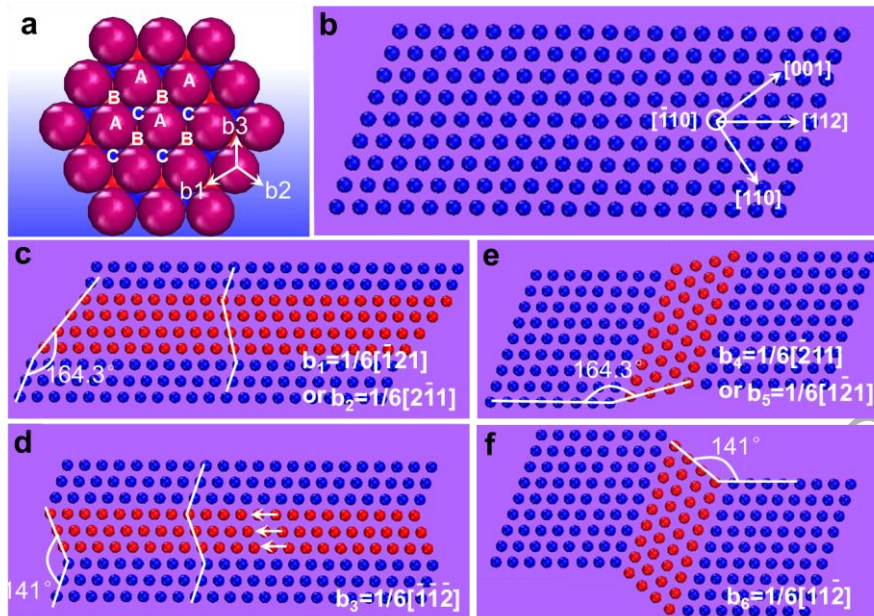


Figure 1. (a) The magnitude and orientation of the three partial dislocations with Burgers vectors, b_1 , b_2 , and b_3 , on the $(\bar{1}\bar{1}1)$ plane of closely-packed atoms, and the atomic stacking positions A, B, C. (b) Atomic structure of a perfect FCC structured crystal that viewed along $[110]$ direction. (c) Twin formed by partial dislocations b_1 or b_2 glide on successive $(\bar{1}\bar{1}1)$ planes, the kink angle is 164.3° . (d) Twin formed by partial dislocations b_3 glide on successive $(\bar{1}\bar{1}1)$ planes, the kink angle is 141° . (e) Twin formed by partial dislocations b_4 or b_5 glide on successive (111) planes, the kink angle is 164.3° . (f) The kink angle is 141° while the twin formed by partial dislocations b_6 .

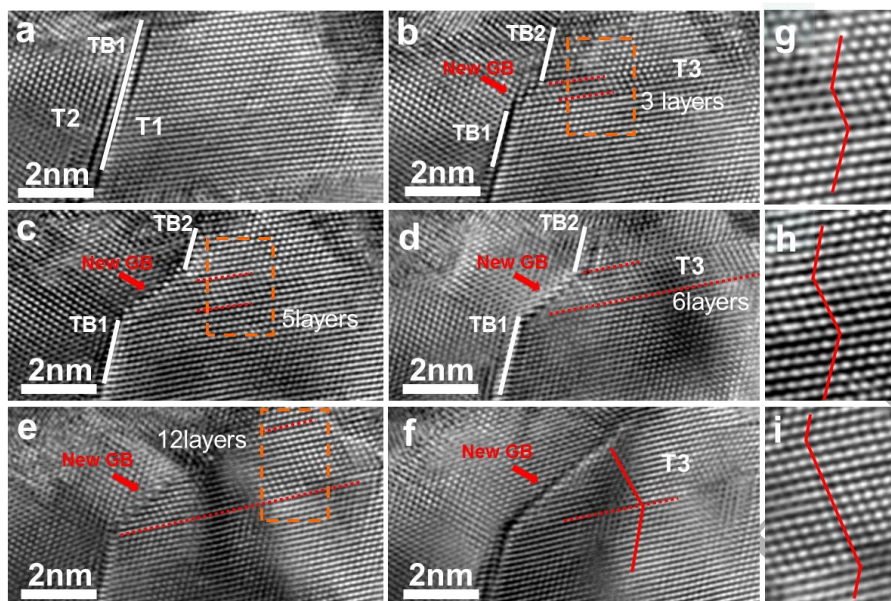


Figure 2. Series of HRTEM images showing the atomic-scale process of the TB-HAGB transition. (a) Grains “1” and “2” are twins and the TB1 is flat. (b) A 3-layered twin is formed in the T1, and the original flat TB1 kinked and changed into a HAGB. (c-f) The twin growth from 5 atomic layers into 6 atomic layers and then eventually several tens of atomic layers, lead to the length of HAGB increase quickly. (g)-(i) Enlarged images corresponding to the red framed region of (b), (c) and (e), respectively, showing the evolution of the atomic structure of the deformation twin.

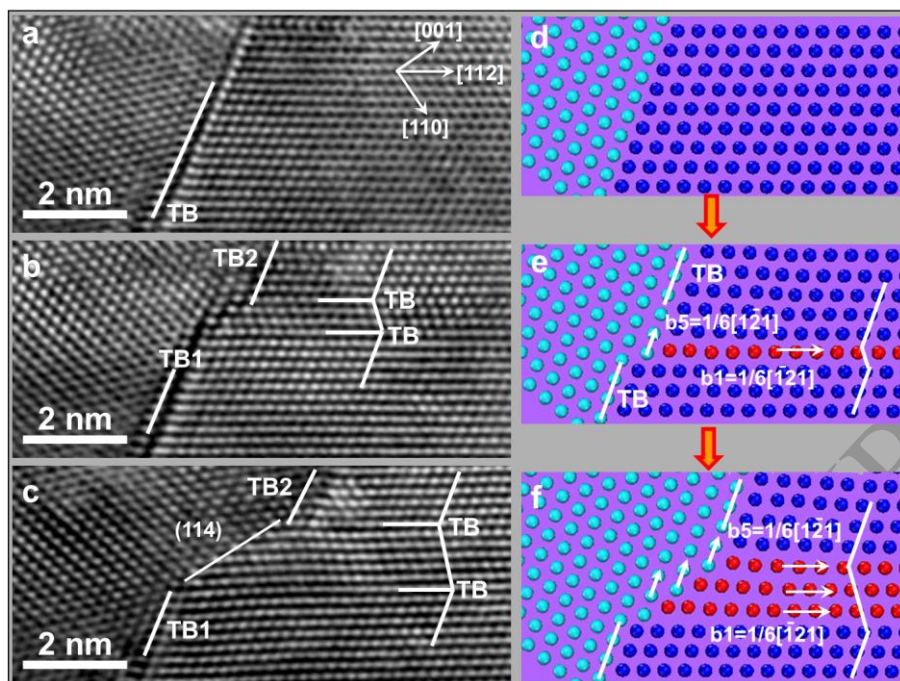


Figure 3. (a-c) Enlarged HRTEM images show the TB-HAGB transition process at atomic scale. As shown in (a) the original TB is flat. (b) With the new twin nucleation and TB2 migration, TB transition into a HAGB. (c) As the new twin growth, the length of HAGB increase correspondingly. (d) The atomic configurations show that the TB is flat before plastic deformation. (e) Partials b_1 or b_2 nucleated from the TB react with the partials b_4 or b_5 nucleated from the same sites. (f) Repetition of the above dislocation nucleation and reaction process leads to the transformation of the TB into a HAGB.

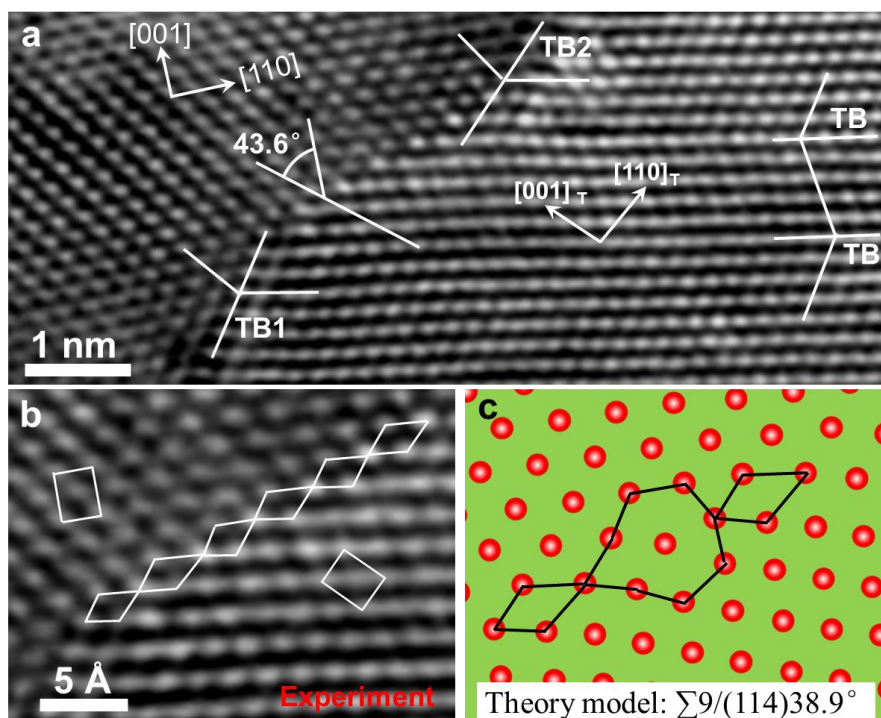
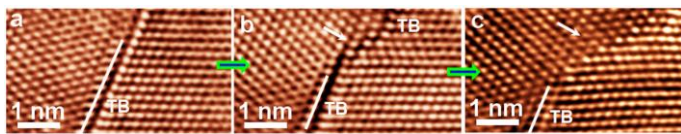


Figure 4. (a) Typical HRTEM image shows the atomic-scale structure of the newly formed $\Sigma 9/(114)$ HAGB. The measured GB angle is 43.6° , which is $\sim 4.7^\circ$ larger than the theoretical values of 38.9° . (b) Enlarged HRTEM image shows the structural unit of the newly formed $\Sigma 9/(114)$ HAGB. (c) The atomic configuration of the theoretic $\Sigma 9/(114)$ GB structure.

Graphical Abstract

ACCEPTED MANUSCRIPT